PNAS

Supporting Information for
BAP1 is a novel regulator of HIF-1α.

Angela Bononi[1], Qian Wang[2,3], Alicia A. Zolondick[1,4], Fang Bai[2,5], Mika Steele[1], Joelle S. Suarez[1], Sandra Pastorino[1], Abigail Sipes[1], Valentina Signorato[1], Angelica Ferro[1], Flavia Novelli[1], Jin-Hee Kim[1], Michael Minaai[1,4], Yasutaka Takinishi[1], Laura Pellegrini[1], Andrea Napolitano[1], Ronghui Xu[1], Christine Farrar[1], Chandra Goparaju[1], Cristian Bassi[6], Massimo Negrini[6], Ian Pagano[1], Greg Sakamoto[1], Giovanni Gaudino[1], Harvey I. Pass[6], Jose N. Onuchic[2,*], Haining Yang[1,*], and Michele Carbone[1,*]

A.B.[1] and Q.W.[2,3] contributed equally to this work.
*Michele Carbone, MD, PhD, Haining Yang, MD, PhD, Jose N. Onuchic, PhD.
Email: mcarbone@cc.hawaii.edu, haining@hawaii.edu, jose.onuchic@rice.edu

This PDF file includes:

Supporting Information Text

Materials and Methods

Immunohistochemistry
Forty-two MM formalin-fixed paraffin-embedded tissue slides were obtained from the National Mesothelioma Virtual Bank (NMVB) at the University of Pittsburgh and used for BAP1 and HIF-1α IHC analyses. IHC analysis of BAP1 protein expression was performed as previously described using a mouse monoclonal anti-BAP1 antibody (C-4: Santa Cruz Biotechnology) (1); IHC analysis of HIF-1α protein expression was performed as using a rabbit polyclonal anti-HIF-1α antibody, dilution 1:200 (Hi pH) (NB100-479, Novus Biologicals). Specimens were de-identified before analysis and experiments were conducted by investigators and analyzed by a board-certified pathologist with extensive experience in MM diagnosis (MC) blinded to the mutation status of the samples. The two germline *BAP1* mutated biopsies were donated to us by the patients.

Cell cultures
Human dermal skin fibroblasts from explants of skin biopsies were collected, as previously described (2). Fibroblasts were cultured in Dulbecco modified Eagle's medium (DMEM) with glucose (4.5 g/L), 2 mM L-glutamine, without sodium pyruvate (Corning Cellgro, # 10-017-CV), supplemented with 10% fetal bovine serum (FBS) (Seradigm, # 1500-500), and 1% penicillin–streptomycin (PS) (Life Technologies, # 15140-163). Primary human mesothelial (HM) cells were obtained from pleural effusions of individuals with non-malignant conditions and cultured in DMEM with 20% FBS and 1% PS, as previously described (3). Human embryonic kidney 293 cells (HEK-293) were cultured in DMEM supplemented with 10% FBS and 1% PS. Cells were cultured in a humidified atmosphere of 5% (v/v) carbon dioxide in air at 37 °C.
For experiments performed in hypoxic conditions, cells were cultured for the indicated time in the InvivO2 400 workstation (The Baker Company, Model RUS.CMVI402) at 37°C, with 5% CO_2, 94% N_2, and 1% O_2 (unless otherwise specified).
All cells used in the experiments were routinely tested for mycoplasma contamination using LookOut Mycoplasma PCR Detection Kit (Sigma-Aldrich, cat no. MP0035) and were confirmed to be mycoplasma-free. Experiments were conducted in triplicate.

Gene silencing with siRNA, adenovirus-mediated gene transfer, and transfection
siRNA oligonucleotides were obtained from Qiagen. GeneSolution siRNAs targeting four different *BAP1* mRNAs: Hs_BAP1_1, cat.no: SI00066696; Hs_BAP1_2, cat.no: SI00066703; Hs_BAP1_3, cat.no: SI00066710; Hs_BAP1_5, cat.no: SI03036390.
Adenoviruses expressing BAP1 and GFP were purchased from SignaGen Laboratories (Ad-BAP1, catalogue number SL175127; Ad-GFP, catalogue number SL100708). Primary human fibroblast cells derived from individuals carrying germline *BAP1* mutations were seeded at 300,000 cells per condition and cultured for 24 hours. Cells were washed once with 1X PBS and the culture media was replaced with fresh culture media at half of the standard volume. Cells were transduced with either Ad-GFP or Ad-BAP1 with 10 MOI per cell for 24 hours. After 24 hours, cells were collected and counted, then 300,000 cells per condition were reseeded into normoxia and hypoxia (1% O_2) conditions for 6 hours, and collected for lysis. Expression plasmids for Myc-BAP1, Myc-BAP1(W), Myc-BAP1(L), Myc-BAP1(C91S), and the Myc-tagged BAP1 fragments [Myc-BAP1(UCH), aa: 1-240; Myc-BAP1(NORS), aa: 240-598, Myc-BAP1(CTD-NLS), aa: 598-729; Myc-BAP1(UCH-NORS-CTD), aa: 1-699; Myc-BAP1(UCH-NORS), aa: 1-598; Myc-BAP1(NORS-CTD-NLS), aa: 240-729] were produced by Blue Heron Biotech and previously described (2). Expression plasmids for Myc-BAP1(mut), the HA-tagged human HIF-1α fragments and point mutations plasmids [HA-HIF-1α(74-826), HA-HIF-1α(2-400), HA-HIF-1α(401-826), HA-HIF-1α(mut), HA-HIF-1α(I675A), HA-HIF-1α(F678A), HA-HIF-1α(I679A), HA-HIF-1α(L691A)] and the Flag-HIF-1β fragments [Flag-HIF-1β(2-470), Flag-HIF-1β(42-470), Flag-HIF-1β(471-789), Flag-HIF-1β(582-789)] were custom produced by Blue Heron Biotech. pCMV6-AN-Myc (cat. no. PS100012) and human-HIF-1alpha-Myc-Flag (cat. no. RC202461) were purchased from Blue Heron Biotech. The following plasmids were purchased from Addgene: Flag-HA-pcDNA3.1 (cat. no. 52535), HA-Ubiquitin (cat. no. 18712), HA-HIF-1α (cat. no. 18949), Flag-HIF-1β (cat. no. 99916). HEK-293 cells were cultured for 24 hours, transiently transfected using polyethylenimine (PEI) and used in the experiments 24 hours post-transfection.

Quantitative Real-Time PCR
Total RNA was extracted by the RNeasy Plus Mini Kit (Qiagen, #74134) and quantified by spectrophotometric analysis. RNA integrity and concentration was assessed using the Agilent 2100 BioAnalyzer. cDNA was synthesized using the High-Capacity cDNA Reverse Transcription Kit (Applied Biosystems, cat no. 4368814) following the manufacturer's instructions. Quantitative real-time PCR was performed in triplicate using TaqMan® Universal Master Mix II (Applied Biosystems, cat no. 4440040) and a commercially available TaqMan Probes (*HIF1A*, ThermoFisher Scientific, cat no. Hs00153153_m1) on a StepOnePlus system (Applied Biosystems). The mRNA levels were normalized using the geometric mean of three reference genes (18S and β-actin).

Western blot (WB)
Total cell lysates were prepared in M-PER (Thermo Scientific, cat. no. 78501) reagent supplemented with proteases and phosphatases inhibitors [2 mM Na_3VO_4, 2 mM NaF, 1 mM PMSF and protease inhibitor cocktail], and 1 mM DTT. For hypoxic cell culture, cells were harvested under hypoxic conditions; briefly, cells were washed once with cold PBS and then harvested by scraping followed by centrifugation at 16,000 x g for 1 min.
Protein extracts were quantified using the Bradford assay (Bio-Rad Laboratories); 15 µg of proteins were loaded and separated on NuPAGE® Novex 4-12% Bis-Tris Gel (Life Technologies), and electron-transferred to PVDF membrane according to standard procedures.
Primary antibodies used were: BAP1 (C-4) (Santa Cruz Biotechnology, cat. no. sc-28383), BAP1 (D7W70) (Cell Signaling, cat. no. 13271), HIF-1α (BD Bioscience, cat. no. 610959), HIF-1β (Cell Signaling, cat. no. 5537), Myc-Tag (9B11) Mouse mAb (HRP Conjugate) (Cell Signaling, cat. no. 2040); α-Tubulin (4G1) (Santa Cruz Biotechnology, cat. no. sc-58666), Ubiquitin (P4D1) Mouse mAb (HRP Conjugate) (Cell Signaling, cat. no. 14049), VHL (Santa Cruz Biotechnology, cat. no. sc-135657). Secondary antibodies used were: Goat anti-Mouse IgG (H+L) Secondary Antibody, HRP (Thermo Scientific, cat. no. 32430); Goat anti-Rabbit IgG (H+L) Secondary Antibody, HRP (Thermo Scientific, cat. no. 32460).

Co-immunoprecipitation
Where indicated, cells were incubated in hypoxic conditions and harvested as described above. HEK-293 cells were transiently transfected using polyethylenimine and collected 24 hours later; Cells were lysed in buffer containing 50 mM Tris, at pH 7.5, 150 mM NaCl, glycerol 10%, 1 mM EDTA, 50 mM NaF and NP-40 0.1%, supplemented with protease inhibitor cocktail, 2 mM Na_3VO_4, 50 nM Okadaic Acid (OA), 1 mM PMSF and protease inhibitor cocktail, and 1 mM DTT. Proteins were extracted and pre-cleared by incubating lysates with A or G-coated (depending on the species of the primary antibody used in the CoIP, mouse and rabbit respectively) Sepharose beads (GE Healthcare), for 1 hour at 4°C.
For endogenous CoIP of BAP1 and HIF-1α, the supernatants (700 µg, referred as "Input") were incubated overnight with 10 µg/mg BAP1 Antibody (Bethyl Laboratories, cat. no. A302-242A) at 4 °C; precipitation of the immune complexes was performed with A-coated sepharose beads for 3 hours at 4 °C, according to manufacturer's instructions.
For exogenous CoIP in HEK-293 cells expressing Myc-, Flag-, of HA-tagged proteins, supernatant was incubated for 3 hours at 4 °C with Ezview™ Red Anti-c-Myc Affinity Gel (Sigma-Aldrich, cat. no. E6654), Ezview™ Red ANTI-FLAG® M2 Affinity Gel, clone M2 (Sigma-Aldrich, cat. no. F2426), or Ezview™ Red Anti-HA Affinity Gel (Sigma-Aldrich, cat. no. E6779), respectively. After immunoprecipitation, the beads were washed three times with lysis buffer, at 4 °C, and suspended in 40 µl of 2X Laemmli buffer. 10-20 µl (depending on experiment) were loaded on the gel and the samples were processed by SDS-PAGE and analyzed by WB.

***In vitro* ubiquitylation and de-ubiquitylation assays**
In vitro ubiquitylation and de-ubiquitylation assays were performed as previously described (2).

Duolink Proximity Ligation Assay
IBIDI µ-Slide VI 0.4 ibiTreat sterile slides (IBIDI catalog number: 80606) were coated with 0.13mM human plasma fibronectin purified protein (Sigma-Aldrich catalog number: FC010) for 1 hour at room temperature. *BAP1*^{WT} and *BAP1*$^{+/-}$ fibroblasts were seeded at a density of 2 x 10^5 cells per channel in 10% FBS DMEM medium and were placed in 1% oxygen chamber at 37°C for 6 hours. Cells were fixed in 4% formaldehyde for 15 minutes in 1% oxygen at 37°C, and then washed in PBS. Cells were permeabilized with 0.1% Triton

X-100 (v/v in PBS) for 10 minutes at room temperature. Unspecified binding sites were blocked with Duolink In Situ Proximity Ligation Assay (PLA) blocking solution from the Duolink In Situ Red Starter Kit Mouse/Rabbit (Sigma-Aldrich catalog number: DUO92101) overnight at 4°C. Cells were incubated overnight at 4°C with primary antibodies specific for BAP1 (Santa Cruz Biotechnology catalog number: sc-28383) and HIF-1α (Novus Biologicals catalog number: NB100-479) in an antibody diluent buffer from the Duolink PLA kit. Detection was performed following the manufacturer's protocol. Cells were incubated at 37°C for 1 hour with fluorescent probes from the Duolink PLA kit conjugated to mouse and rabbit. Cells were washed 5 times for 5 minutes with 1x Duolink In Situ Wash Buffer A and a ligation-ligase solution was added to each sample for 30 minutes at 37°C.Cells were washed 5 times for 5 minutes with 1x Duolink In Situ Wash Buffer A and an amplification-polymerase solution was added to each sample for 100 minutes at 37°C, washed twice for 10 minutes with 1X Duolink In Situ Wash Buffer B, and then twice in 0.01X Duolink In Situ Wash Buffer B for 1 minute. Duolink In Situ Mounting Medium with DAPI was applied to each sample. Protein-protein interactions appeared as red dots using the Leica Thunder Live Cell 3D microscope. Images were processed and cells showing nuclear BAP1–HIF-1α red dots were counted using the Analyze Particles ImageJ software plugin.

Computational modeling the CTD and the NLS domain of BAP1

We performed coarse-grained molecular dynamics simulations to predict the structure of the CTD and the NLS domain of BAP1 (noted as "BAP1(CTD-NLS)") by using the AWSEM force field (4). The initial structure of BAP1(CTD-NLS) was set to a random extended chain. Next, the simulating annealing procedure was performed to gradually quench the system from 500K to 300K within 4 million steps. The time step was set to 5 fs. This procedure was repeated 20 times. The predicted 20 binding complex structures were collected and clustered using a clustering algorithm based on a local relative similarity order parameter mutual Q (5). The center of the largest structure was chosen as the final predicted binding complex. To verify this structural model, we also used two widely used protein structure predicting methods, I-TASSER and RaptorX (6-9), to predict the structure of BAP1(CTD-NLS).

Computational modeling the binding complex of BAP1 and HIF-1α

Three methods were used to study the binding complex between BAP1 and HIF-1α. First, a rigid molecular docking protocol was applied to predict the structure of the CTD of BAP1 and HIF-1α in the presence of DNA by using the Cluspro server (10-12). The structure of the CTD of BAP1 comes from the computational modeling described above. The structure of the HIF-1α – DNA complex comes from its crystal structure (PDB ID: 4zpr) (13). Second, the interfacial contacts between BAP1 and HIF-1α were predicted by the RaptorX server (14). Third, ab initio coarse-grained molecular dynamic simulations were performed to study the binding kinetics between BAP1(CTD-NLS) and residues 1-73 of HIF-1α (noted as "HIF-1α-r73") in the presence of DNA by using the AWSEM force field (15). The initial distance between BAP1(CTD-NLS) and the HIF-1α-r73-DNA complex was set to 150 Å. Unbiased Langevin dynamic simulations were performed to study how BAP1-CN kinetically binds to the HIF-1α-r73-DNA complex. The temperature was set to 300K. Each trajectory last 40 million steps while the time step was set to 5 fs. This protocol was repeated 20 times.

Supplementary Figure 1

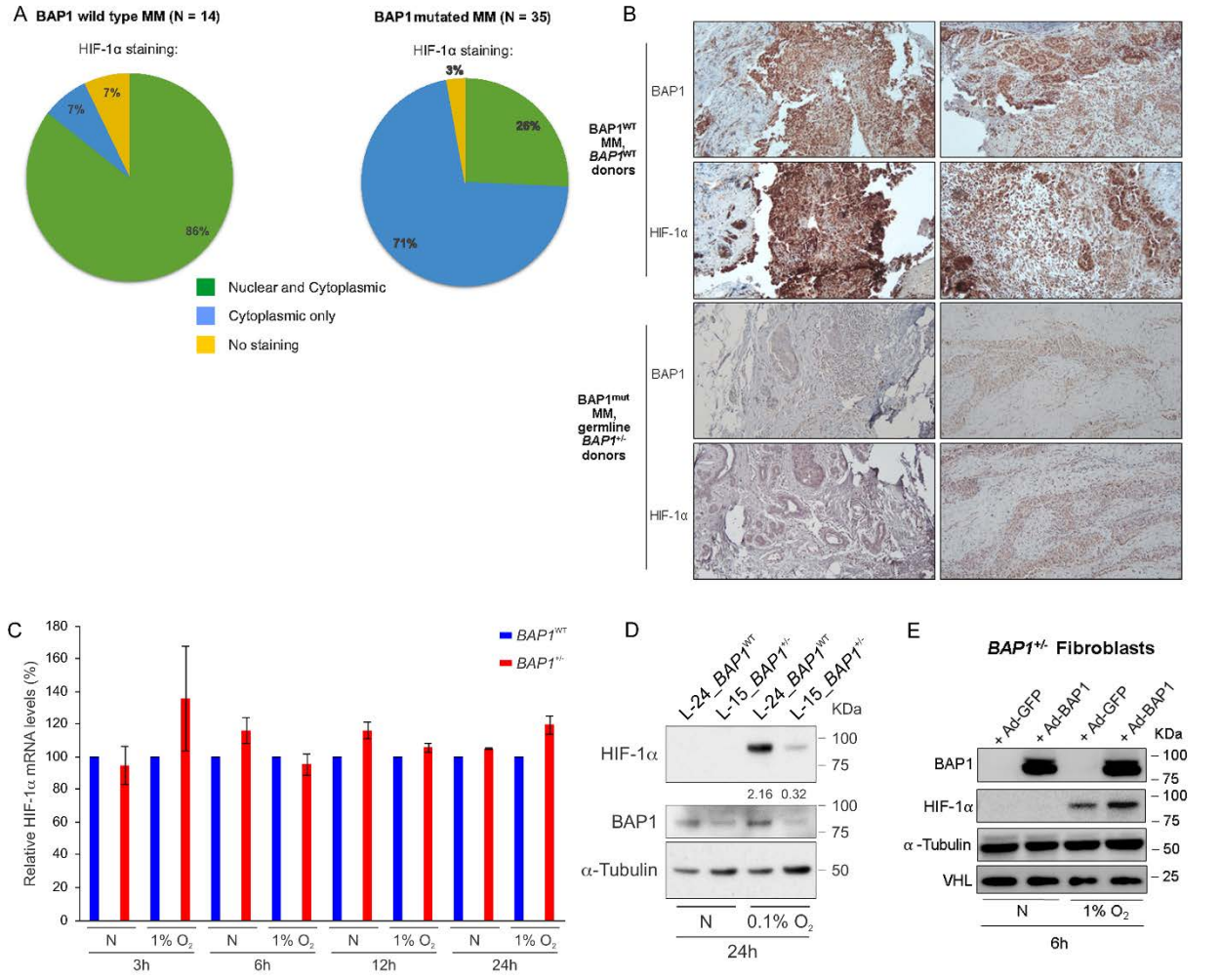

Fig. S1. BAP1 regulates HIF-1α protein levels. (**A**) Pie chart depicting the percentages of HIF-1α nuclear and cytoplasmic immunostaining (green), cytoplasmic only immunostaining (blue), or no immunostaining (yellow), in *BAP1*^{WT} mesotheliomas (left, N = 14) and *BAP1* mutated mesotheliomas (right, N = 35) from the NMVB (related to Figure 1A). (**B**) BAP1 and HIF-1α immunostain of 2 sporadic mesothelioma biopsies with BAP1^{WT} (top two) and 2 mesotheliomas biopsies with BAP1$^{-/-}$ from 2 individuals carrying germline BAP1 mutation: their cells in the tumor microenvironment are BAP1$^{+/-}$ (bottom two). Note absent HIF-1α stain in the nuclei of the tumor cells and marked reduction in the tumor microenvironment of BAP1 mutated mesotheliomas compared to BAP1^{WT}. (**C**) Quantitative PCR analysis of *HIF1A* mRNA expression levels in *BAP1*^{WT} and *BAP1*$^{+/-}$ primary fibroblasts incubated in normoxia (N) or hypoxia (1% O_2) for the indicated times. *HIF1A* mRNA expression levels were normalized using the geometrical mean of 18S and ACTB reference genes. Data shown as mean ± s.d. of n = 2 biological replicates per condition, representative of two independent experiments. (**D**) Immunoblot: amounts of HIF-1α protein in total cell lysates of L fibroblasts, matched by gender and age, incubated in 0.1% O_2 for 24 hours.

Supplementary Figure 2

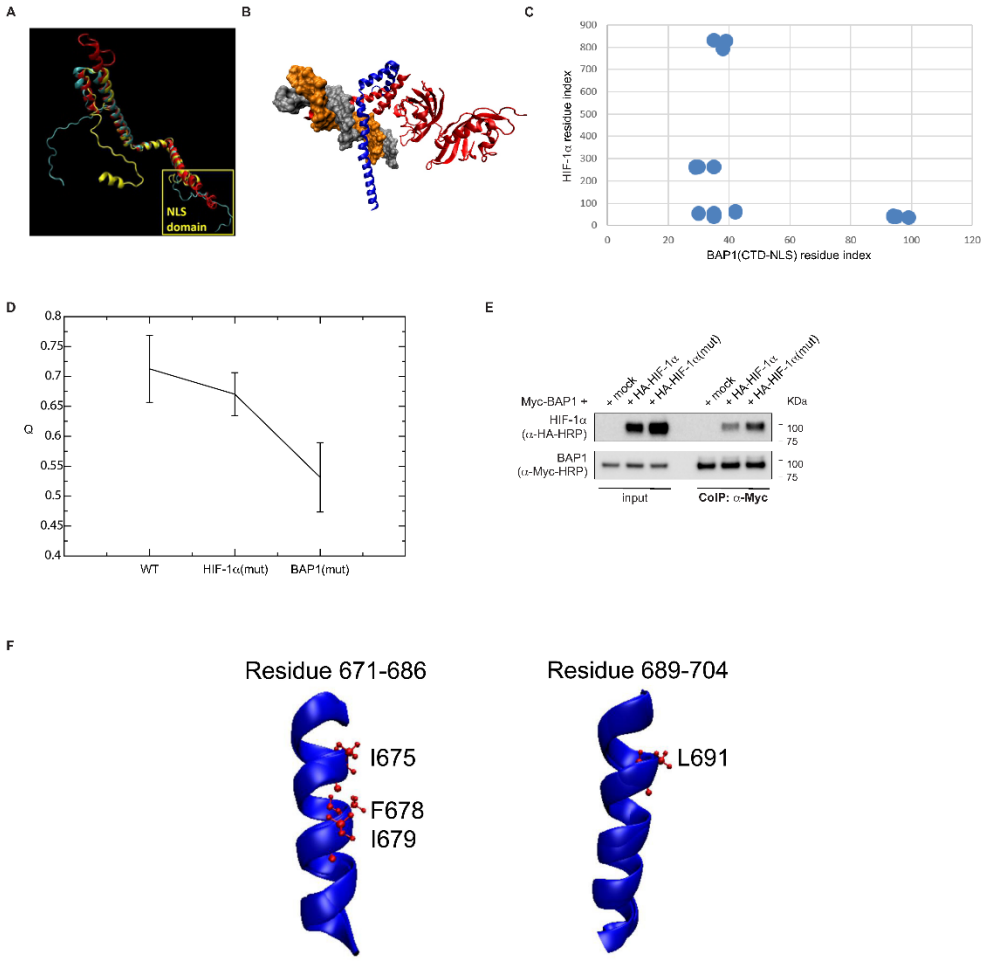

Fig. S2. Modelling of the BAP1-HIF-1α interaction. (A) Structural modeling for the CTD domain and the NLS domain of BAP1 using three different methods: red, the prediction by molecular dynamic simulations; cyan, the prediction by the RaptorX server (9); yellow, the prediction by the I-TASSER server (6-8). (B) Structural modeling for the binding complex of the CTD domain of BAP1 (blue) and HIF-1α (red, PDB ID: 4zpr) in the presence of DNA (orange and grey) by the ClusPro server (10-12). (C) Top 20 interfacial residue-residue contact predictions between BAP1(CTD-NLS) and HIF-1α, predicted by the RaptorX server (14). (D) The fraction of the interfacial contact (Q) in simulations for the wide-type BAP1-HIF-1α binding complex, as well as two mutation sets: HIF-1α(mut) (mutating F37, L40, Q43, L44 of HIF-1α to ALA) and BAP1(mut) (mutating I675, F678, I679 and L691 of BAP1 to ALA). Each case was simulated 20 times and the averaged results are shown here; higher Q means higher structural similarity to the model in Figure 3A in the main text. (E) Point mutations of residues F37, L40, Q43, L44 of HIF-1α do not affect the binding with BAP1. CoIP of BAP1 and HIF-1α in homogenates from HEK-293 cells co-transfected with Myc-BAP1 and HA-tagged HIF-1α, or HIF-1α (mut), or empty vector (mock); anti-Myc resin was used as bait. (F) Structure superposition of WT BAP1 and BAP1 with four mutations (I675, F678, I679 and L691) after 500-ns all-atomistic simulations.

Supplementary Figure 3

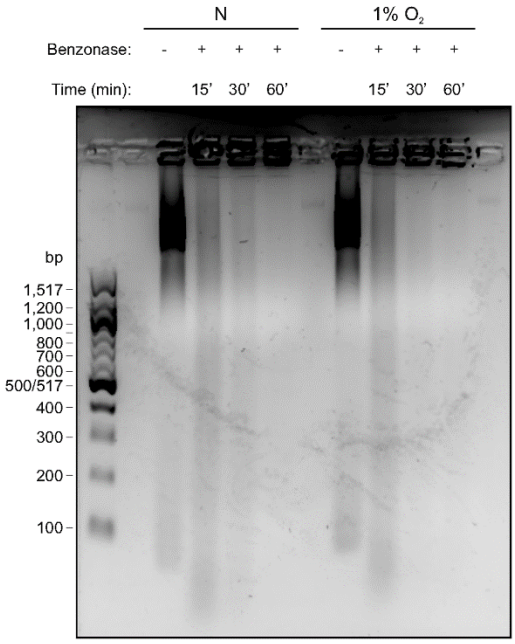

Fig S3. DNA degradation with benzonase. HEK-293 cells were grown in normoxia (N) or hypoxia (1% O_2) for 4 hours. Cell homogenates were collected, treated with benzonase for 15, 30 or 60 minutes, and then used for CoIP experiments (Figure 4E). Agarose gel showing progressive DNA degradation in HEK-293 cell homogenates treated with 500 U of benzonase for the indicated time.

SI References

1. M. Nasu *et al.*, High Incidence of Somatic BAP1 alterations in sporadic malignant mesothelioma. *Journal of thoracic oncology : official publication of the International Association for the Study of Lung Cancer* **10**, 565-576 (2015).
2. A. Bononi *et al.*, BAP1 regulates IP3R3-mediated Ca(2+) flux to mitochondria suppressing cell transformation. *Nature* **546**, 549-553 (2017).
3. M. Bocchetta *et al.*, Human mesothelial cells are unusually susceptible to simian virus 40-mediated transformation and asbestos cocarcinogenicity. *Proceedings of the National Academy of Sciences of the United States of America* **97**, 10214-10219 (2000).
4. M. Chen *et al.*, Template-Guided Protein Structure Prediction and Refinement Using Optimized Folding Landscape Force Fields. *J Chem Theory Comput* **14**, 6102-6116 (2018).
5. M. Chen, X. Lin, W. Lu, J. N. Onuchic, P. G. Wolynes, Protein Folding and Structure Prediction from the Ground Up II: AAWSEM for alpha/beta Proteins. *J Phys Chem B* **121**, 3473-3482 (2017).
6. A. Roy, A. Kucukural, Y. Zhang, I-TASSER: a unified platform for automated protein structure and function prediction. *Nat Protoc* **5**, 725-738 (2010).
7. J. Yang *et al.*, The I-TASSER Suite: protein structure and function prediction. *Nat Methods* **12**, 7-8 (2015).
8. J. Yang, Y. Zhang, I-TASSER server: new development for protein structure and function predictions. *Nucleic Acids Res* **43**, W174-181 (2015).
9. M. Kallberg *et al.*, Template-based protein structure modeling using the RaptorX web server. *Nat Protoc* **7**, 1511-1522 (2012).
10. S. Vajda *et al.*, New additions to the ClusPro server motivated by CAPRI. *Proteins* **85**, 435-444 (2017).
11. D. Kozakov *et al.*, The ClusPro web server for protein-protein docking. *Nat Protoc* **12**, 255-278 (2017).
12. D. Kozakov *et al.*, How good is automated protein docking? *Proteins* **81**, 2159-2166 (2013).
13. D. Wu, N. Potluri, J. Lu, Y. Kim, F. Rastinejad, Structural integration in hypoxia-inducible factors. *Nature* **524**, 303-308 (2015).
14. S. Wang, S. Sun, Z. Li, R. Zhang, J. Xu, Accurate De Novo Prediction of Protein Contact Map by Ultra-Deep Learning Model. *PLoS Comput Biol* **13**, e1005324 (2017).
15. A. Davtyan *et al.*, AWSEM-MD: protein structure prediction using coarse-grained physical potentials and bioinformatically based local structure biasing. *J Phys Chem B* **116**, 8494-8503 (2012).